Shock Waves @ Marseille IV

Springer
Berlin
Heidelberg
New York
Barcelona
Budapest
Hong Kong
London
Milan
Paris
Tokyo

R. Brun L. Z. Dumitrescu (Eds.)

Shock Waves @ Marseille IV

Shock Structure and Kinematics, Blast Waves and Detonations

Proceedings
of the 19th International Symposium
on Shock Waves
Held at Marseille, France, 26-30 July 1993

With 434 Figures

Springer

Professor Dr. Raymond Brun

Professor Dr. Lucien Z. Dumitrescu

Université de Provence, Centre Saint-Jérôme
IUSTI-MHEQ, Case 321, F-13397 Marseille Cedex 20, France

The Preface and lists of the Symposium Committees and of the Sponsoring Organisations are printed in Volume I.

ISBN-13:978-3-642-79534-3 e-ISBN-13:978-3-642-79532-9
DOI: 10.1007/978-3-642-79532-9

CIP data applied for

Typesetting: Camera ready by editors
SPIN: 10467571 55/3144 - 5 4 3 2 1 0 - Printed on acid-free paper

Contents - Volume IV*

* The Contents of the other volumes are given at the end of the book

Part 2: Shock Reflection and Diffraction

Part 3: Shock - Interface Interactions

Part 4: Interactions Involving Shocks

Part 5: Explosions, Blast Waves, Detonations

Survey Paper

Plenary Lectures

Volume IV: Shock Structure and Kinematics. Blast Waves and Detonations - An Introductory Survey

L.F. Henderson
Dept. of Mechanical Engineering, Univ. of California - Berkeley, CA 94720, USA

1. The Riemann Problem

This problem was defined by Courant and Friedrichs (1948) in their famous book. A Riemann problem is an initial value problem for a system of conservation laws, such that the initial data is scale invariant. The conservation laws have hyperbolic character, and the invariance refers to the fact that there is no length or time scale in the initial data. Riemann's (1860) theory of the shock tube is the quintessential example of the one-dimensional problem, while shock reflection, refraction and diffraction are examples of two-dimensional Riemann problems.

2. The equation of state (EOS)

Many researchers have found that the EOS of a material has a profound effect on the nature of the shock phenomena. The greatest of the earlier papers was undoubtedly written by Bethe (1942). Much of what has happened since has been discussed in an excellent review by Menikoff and Plohr (1989). This work has led to a means for classifying EOS's into types that obey certain restrictions. Before describing them, it will be convenient to introduce the thermodynamic properties that will be needed.

3. The thermodynamic properties

The properties which are of the greatest importance are as follows:

The adiabatic exponent
$$\hat{\gamma} \equiv \frac{V}{P}\left.\frac{\partial^2 E}{\partial V^2}\right|_S = -\frac{V}{P}\left.\frac{\partial P}{\partial V}\right|_S = \frac{a^2}{PV} = \frac{1}{K_S}$$

The Grüneisen coefficient
$$\Gamma \equiv -\frac{V}{T}\frac{\partial^2 E}{\partial S \partial V} = \frac{\beta V}{C_V K_T}$$

The dimensionless specific heat
$$g \equiv \frac{PV}{T^2}\left.\frac{\partial^2 E}{\partial S^2}\right|_V = \frac{PV}{C_V T}$$

The fundamental derivative
$$G \equiv -\frac{1}{2}V\frac{\partial^3 E/\partial V^3|_S}{\partial^2 E/\partial V^2|_S} = \frac{1}{2}\frac{V^2}{\hat{\gamma}P}\left.\frac{\partial^2 P}{\partial V^2}\right|_S$$

where E is energy, V volume, S is entropy, P is pressure, T is temperature, and:

$$K_S \equiv -\frac{1}{V}\left.\frac{\partial V}{\partial P}\right|_S \quad \textit{is isentropic compressibility}$$

$$K_T \equiv -\frac{1}{V}\left.\frac{\partial V}{\partial P}\right|_T \quad \textit{is isothermal compressibility}$$

$$\beta \equiv \frac{1}{V}\left.\frac{\partial V}{\partial T}\right|_P \quad \textit{is coefficient of thermal expansion}$$

Shock Waves @ Marseille IV
Editors: R. Brun, L. Z. Dumitrescu

4. The standard Riemann theory

This was inaugurated by Bethe. In present day usage its strongest form occurs when the EOS obeys the conditions:

$$G > 0 \qquad \text{and} \qquad \Gamma \leq \frac{PV}{E} \Rightarrow 1 + \frac{1}{2}\Gamma\frac{\Delta V}{V} > O$$

When $G > 0$, then by definition the isentropics are strictly convex in the (V, P) plane. This condition is obeyed by nearly all compressible materials when they are in a single phase state, except possibly near a phase boundary. When in addition the condition on Γ is satisfied, which is called the strong condition, then the Hugoniot is also convex in the (V, P) plane. The perfect gas EOS obeys both conditions. Violation of the strong condition occurs for dissociating and/or ionizing gases. When this happens the shock can develop a transverse or ripple instability. When the $G > 0$ condition is violated the shock may develop a splitting instability. When both conditions are satisfied, one finds that the solution of the Riemann problem exists, is unique and stable.

Uniqueness is determined in the (u, P) plane by virtue of the boundary conditions at the contact surface which is present in most Riemann problems, that is

$$\Delta u = 0, \qquad \Delta P = 0$$

where u is the particle speed at the rear of the wave. Uniqueness exists if the wave curves (Hugoniots, isentropics) are convex in the (u, P) plane, so that they intersect at a single point and satisfy the boundary conditions at the intersection. Uniqueness actually requires somewhat less restrictive conditions, namely:

$$G > 0, \qquad \text{and} \quad \Gamma \leq \hat{\gamma}$$

where the latter is called the medium condition which is obeyed by all materials except possibly by liquids of high heat capacity. The weak condition:

$$\Gamma \leq 2\hat{\gamma}$$

is also useful and is obeyed by all known materials. The cited references show that, when

$$G > 0 \qquad \text{then} \qquad \textit{strong} \Rightarrow \textit{medium} \Rightarrow \textit{weak}$$

5. Principle tools for shock wave research

5.1. Computational Fluid Dynamics (CFD)

While numerical methods scarcely existed when the first **Shock Wave Symposium** was held, they are now of crucial importance to our research. Many papers in the present volume use CFD, and especially the second-order Godunov code and the TVD method. The assumptions of the standard theory described above are often implicit in the implementation of the codes. This is automatic for example when the perfect gas EOS is used. Consequently the code may fail to detect say a shock splitting instability near a phase boundary, or a transverse instability in a dissociating or ionizing gas.

Many codes use Euler's equations, which of course neglect the effects of viscosity. It seems very difficult at present to write a code that gives convincing results for the Navier-Stokes equations where shock waves are present. All too often numerical viscosity dominates real viscosity. I suspect that by the Caltech Symposium in 1995 these problems will be overcome. It is well known that the N-S equations underestimate the shock thickness when the shock Mach number $M > 1.5$, approximately. In the papers by Elizarova and Yu, and by Woods et al. this is discussed and alternative methods are developed. However, for dense gases, the length scale introduced by the

shock thickness would be too small to be of much consequence. Rather remarkably the Euler equations can give results that agree well with experiment even in the presence of rather massive boundary layer separation as the results of Hillier's paper demonstrate.

5.2. Mathematical analysis

There seems to be a resurgence of interest in analytically solving a system of partial differential equations associated with Riemann problems, and particularly to those associated with weak Mach reflections, now called von Neumann reflections. I hope that the Caltech Symposium will have a session on "Shock Waves and Riemann Problems" or something like it. However there are no such papers in this volume so I will say no more.

5.3. Experimental results

Among the most important advances in recent years has been the development of holographic interferometry. It works for transparent gases and liquids, and has the advantage of being non-invasive. Some splendid examples were presented by Takayama in his Paul Vieille plenary lecture; some of them are published in this volume. The size of pressure transducers has dropped by about one order of magnitude during the same period, so that finer resolution of pressure-time signatures is now possible. Unfortunately, we still need them to be much smaller than can be achieved at present.There has also been outstanding development in nano-second technology and in signal processing. The advent of charge-coupled devices (CCD) will be a boom to processing shock wave data as their resolution improves.

These steady improvements are continually applied to a number of long-standing shock wave problems that are still in dispute, as subsequent pages will show. Experimenters continue to study shock phenomena at ever more extreme conditions, for example the paper by Grun, where pellets are exploded with lasers, and that by Murakami et al. on thermal shocks in superfluid helium.

The invited paper by Haas describes experiments in which shocks propagate from one gas to another, and accelerate the interface between them. The important Richtmyer-Meshkov instability is prominent for head-on acceleration, and one may see Kelvin-Helmholtz roll-ups for more glancing incidence. There is much information in this paper about plane, cylindrical and spherical boundaries.

6. The Sections

IV.1. Shock structure - propagation and focusing

The arduous problem of imploding shocks continues to attract the attention of experimenters, such as Neemeh et al. and Demmig et al., while methods of producing them are considered by Fujiwara et al. The related problem of shock focusing in gases is discussed by Watanabe et al. and in liquids by Isuzugava et al. Other experiments, which are perhaps of more engineering interest, are the propagation of shocks through baffles (Kuhl and Reichenbach) and in IV.2 in compressive corners (Falcovitz et al.), in a trench (Falcovitz et al.) and ejection from a channel (Bazarov et al.).

IV.2. Shock reflection and diffraction

At least six papers in this Section study the von Neumann reflection (VNR); this problem appears to be an emerging subject for vigorous research in analysis, CFD, and in experiment. The paper by Higashino displays a CFD "atlas" of the known strong and weak shock reflections for monatomic and diatomic gases, but not necessarily for more complex gases. He exhibits some interesting graphics on a VNR. Five papers deal with shock diffraction, while others deal with the refraction

of shocks in gases, liquids, and into porous materials. Other topics covered are the influence of viscosity, and of the chemistry of combustible materials in bifurcating shocks.

IV.3. and IV.4 Shock-interface interactions and Interactions involving shocks

These two Sections include 24 papers in all. About half of them are concerned with the famous Richtmyer-Meshkov (RM) instability, which appears at shock-accelerated gas interfaces. There are numerous experiments and CFD studies reported. I noticed especially the fine resolution in the paper by Jacobs et al., the front tracing method in the paper by Grove et al., and the superb holography in the paper by Itaka and Takayama. The difficult problem of measuring temperature and concentration in RM mixing was undertaken by Touat et al., also of note is the "baroclinic boundary layer" work of Newald et al. and there is much else of value.

Shocks interacting with vorticity also get some considerable attention. For example, when the vorticity arises from gas jets, as with Obermeier et al., or from vortex rings: Minota, Brouillette, Ellzey and Henneke, and Takayama et al.

IV.5. Explosions - Blast waves - Detonations

In this Section there is a greater emphasis on engineering problems. For example, blast wave scaling (Dvoinishnikov et al., Kohlberg et al.), pressure loading (Brossard et al.), and underwater explosions (Parmentier). There are some interesting papers on detonations; I liked the one by Dabora on oblique detonations. There are some on solid state detonations, or those involving dusts (Ohyagi et al., Roucou), and on the stability of imploding waves (Oran and De Vore).

Altogether a volume containing much vigorous research.

Optical Flow Visualization of Shock Wave Phenomena (Paul Vieille Memorial Lecture)

K. Takayama
Shock Wave Research Center, Institute of Fluid Science, Tohoku University, 2-1-1 Katahira, Aoba, Sendai 980, Japan

Abstract. Paper presents results of optical flow visualization, mostly of double exposure holographic interferometry applied to various shock wave phenomena at the Shock Wave Research Center of the Institute of Fluid Science, Tohoku University. Topics described here are: 1) shock propagation over perforated walls in air; 2) shock wave interaction with a gaseous interface, a soap bubble filled with helium; 3) three-dimensional visualization of a supersonic flying projectile in air; and 4) underwater shock wave interaction with gas bubbles and gaseous interfaces.

Key words: Optical flow visualization, Shock waves, Reflection, Diffraction, Two-phase flow

1. Introduction

Light waves having a given wavelength are characterised by both wave amplitude and phase. The wave amplitude represents the light intensity, which can be recorded on film by conventional photogrammetry. Dennis Gabor (1948) proposed a unique idea that by superposing monochromatic and coherent light waves, the phase information of the light can be stored on emulsion films and the recorded phase information can be reconstructed later. This is the principle of holography. His invention was originally intended to enhance the magnification of images of electron-microscopes and to improve imaging. In order to succeed with his idea, an intense and coherent light source such as a laser is necessary. However, Gabor managed to construct his first holograms long before the advent of the laser. In 1971, the Nobel prize in physics was bestowed upon him for his invention of holography.

Holography, being intimately supported by the development of commercially available coherent laser sources, has an immense applicability not only to general flow visualizations but particularly to gasdynamic flow visualizations. Russell et al. (1974) and Wortberg et al. (1974) first reported the successful use of holographic interferometry to shock wave research at the Ninth International Shock Tube Symposium, held at Stanford University. Russell et al. (1974) visualized a Ludwieg tube flow. In shock wave research, several successful results of holographic interferometric observations have been reported (Bershader 1987) and today this technique came to routine use (Takayama 1993).

In this Paul Vieille Lecture, applications of double exposure holographic interferometry, mostly to shock tube experiments, are presented, which have been conducted at the Shock Wave Research Center of the Institute of Fluid Science, Tohoku University. The topics are: 1) shock propagation over perforated walls; 2) shock wave interactions with soap bubbles filled with helium; 3) three-dimensional visualization of the flight of a supersonic projectile in air; and 4) underwater shock wave interaction with gas bubbles.

2. Double exposure holographic interferometry

Fig.1 shows a schematic diagram of the image holography set-up for shock tube experiments at the Shock Wave Research Center of the Institue of Fluid Science, Tohoku University. The light source is a Q-switched double pulse ruby laser, Apollo Lasers Ltd. 22HD, 2 J/pulse and 25 ns pulse duration at TEM_{00} mode and wavelength of 694.3 nm. A 6:4 beam splitter divides 60 % of the

Shock Waves @ Marseille IV
Editors: R. Brun, L. Z. Dumitrescu

source light beam into an object beam and 40 % into a reference beam. The object beam, being identical with shadow optics, is expanded by a concave lens and collimated by a Schlieren mirror of 300 mm dia. and 3000 mm focal length and is modulated by the phenomena. The reference beam, designed especially for holography, transports information of the coherent and monochromatic source light and is interfering with the object beam. The difference of light paths of the reference and object beams is adjusted to be not more than 20 mm. In order to satisfy the condition of linear transmittance of holographic emulsion films, the ratio of the object beam to the reference beam is adjusted, by inserting a neutral density filter in the path of the reference beam, approximately from 2:1 to 3:1. Superposition of the reference and object beams can store the phase information of the object beam on holographic emulsion films. When, in addition to the first superposition of the reference and object beams under no-flow conditions, a second exposure is made in synchronization with the shock wave phenomenon, the information stored on the hologram contains the difference of the phase information between these two exposures. The stored image of the phase change is visible in virtual images by a process of so-called reconstruction. The virtual images are then recorded using conventional cameras or video recorders. This is a fundamental difference between the conventional photogrammetry and holographic interferometry.

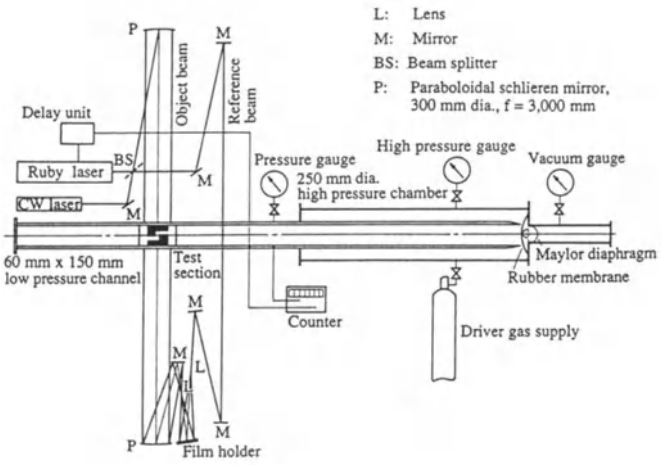

Fig. 1. Optical arrangement of double exposure holographic interferometry

The variations of phase angles during the double exposures are reconstructed as interference fringes so that the correlation between the intensity of the interference fringes and the difference of phase angle $\Delta\phi$ is given by

$$I = A \cos \Delta\phi \tag{1}$$

where A is a constant. If the images of shock wave phenomena are focused, similar to conventional shadowgraphs, on the holographic film by using an image focusing lens, this system is called image holographic inteferometry.

When non-transparent/transparent objects are illuminated by diffused laser beams, the diffused laser beams are modulated by the reflection/transmission from/through the objects. The information of the shape of the objects and the density variation of the flow around the objects is transferred and directly stored by illumination on the holofilm. Unlike the image holograms, no

image lenses are used in this recording method. This system is, therefore, called diffuse holography. Diffuse laser beams which are reflected/transmitted from/through a point of the objects transfer information of this point viewed from different directions. Therefore, by the reconstruction process, three-dimensional information of the objects is recorded.

3. Shock wave propagation over perforated walls

3.1. Shock propagation over slotted double elbows

Shock waves are attenuated when propagating over a perforated or slotted wall. Upon shock reflection over wedges with perforations or over slotted wedges, the critical transition angle of the reflected shock waves from Mach to regular reflections or from regular to Mach reflections was found to be smaller than that over a smooth wedge. Due to the mass suction of the flow behind the incident shock and also due to the losses of momentum and energy, slotted walls are often used to control shock attenuation. In automobile exhaust pipes, wall perforations are effectively used to suppress weak shock waves which result from the coalescence of compression waves exhausted from the engine cylinders.

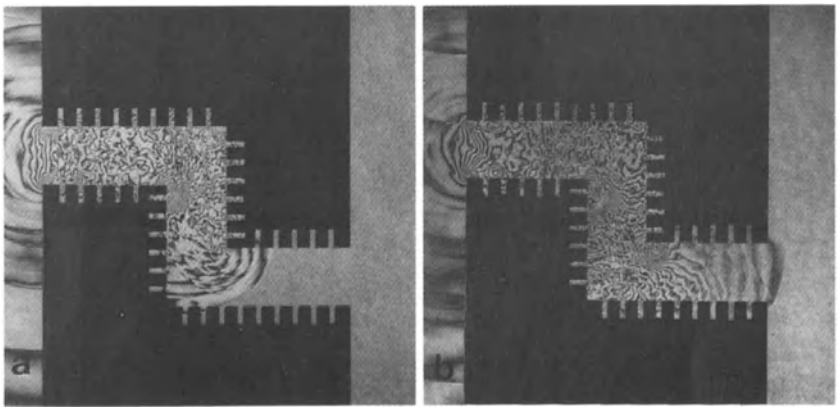

Fig. 2. Shock propagation over a double 90° bend with slotted surface

Fig.2 shows sequential interferograms of shock propagation over double 90° bends with slotted wall surface. The models were installed in a 60 mm × 150 mm shock tube and tested at shock Mach number $M_S = 1.20$ in air.

The shock tube used in the present series of experiments was a so-called diaphragmless shock tube, in which a re-usable rubber membrane was used instead of rupturing diaphragms. The rubber diaphragm was bulged by an auxiliary high pressure gas and separated the test gas from the high pressure driver gas. Upon sudden release of the auxiliary high pressure gas the rubber membrane quickly receded. This is equivalent to the rupture of the diaphragm creating a shock wave in the low pressure channel of shock tubes. As the deformation of the rubber membrane was constrained within its elastic limit and initial conditions of the shock tube were precisely identical, the scatter of resulting shock Mach numbers obtainable in this diaphragmless shock tube was $\pm 0.12\,\%$ for $M_S = 1.02$ to 1.20 (Yang et al. 1993).

Mass suction at individual slits generated expansion waves as seen in Figs.2a and 2b, which caught up the transmitted shock wave propagating along the slotted passage so that this shock wave was well attenuated while propagating. Although details of fringe distributions are slightly

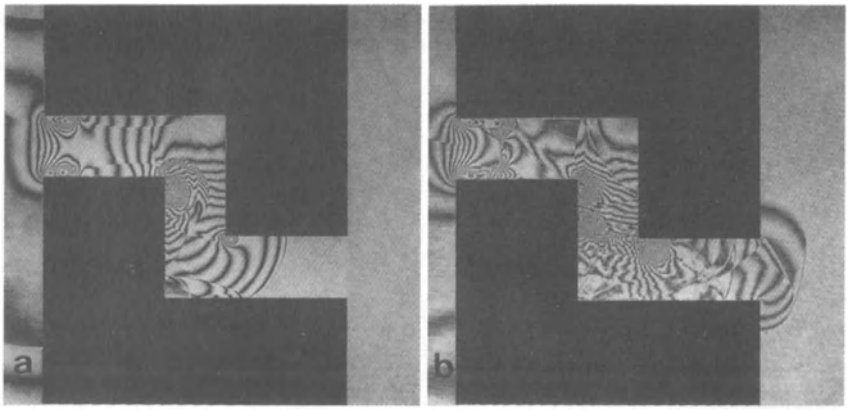

Fig. 3. Shock propagation over a double 90° bend with smooth surface

deviating, TVD finite difference numerical simulations agree reasonably with these interferograms and the resulting shock Mach number at the exit was 1.05 and had an overpressure of only 10 kPa. Figs.3a and 3b exhibit (compare with Fig.2) shock propagation along a double elbow with smooth surface for $M_S = 1.2$ in air. The transmitted shock Mach number at the exit was approximately 1.1 and the corresponding overpressure was 24 kPa.

3.2. Shock interaction over a perforated cylinder

A hollow cylinder, the outer and inner diameters of which were 100 mm and 80 mm, respectively, was installed in a 60 mm × 150 mm shock tube in a 12.5 mm off-centered position as seen in Fig.4a. Slits with 1 mm opening and 1.5 mm separation were distributed over the upper half of the cylinder surface. Fig.4 shows sequential interferograms of a planar shock wave of $M_S = 1.5$ in air propagating over the hollow cylinder.

An interferometric study of shock propagation over a cylinder having a smooth surface has been made experimentally and numerically by Itoh and Takayama (1987). By counting the isopycnics over the cylinder on individual interferograms, corresponding pressure coefficients were experimentally obtained so that unsteady form drag forces were determined. It is found that the unsteady drag force became a maximum when reflected shock transition from regular to Mach reflection occurred at the front surface of the cylinder. Fig.4a shows an earlier stage of shock impingement on the cylinder. The critical transition angle of the reflected shocks is smaller over convex walls with slotted or roughened surfaces.

With propagation over the cylinder, Mach stems appeared both over the smooth surface and slotted surface, as seen in Fig.4b. The mass suction through the slits drove a curved shock wave in the hollow part of the cylinder which was initially convex toward the direction of its propagation. The shape of the curved shock wave gradually became concave when the Mach stem started diffracting along the rear surface of the cylinder in Fig.4c. Consequently, the resulting curved shock wave formed a caustic surface whereby the pressure behind the caustic surface was high. The high pressure was then released reversely through the slits toward outside the hollow cylinder and formed a precursory shock wave. Fig.4d shows the interaction between the precursory shock wave and the diffracting Mach stem.

This is part of a series of experiments related to the investigation of mutual interactions of a shock wave propagating along a solid surface with a precursory wave generated along the solid surface. The present experimental setup shows one of the artificial and unusual cases which can be readily compared with analyses.

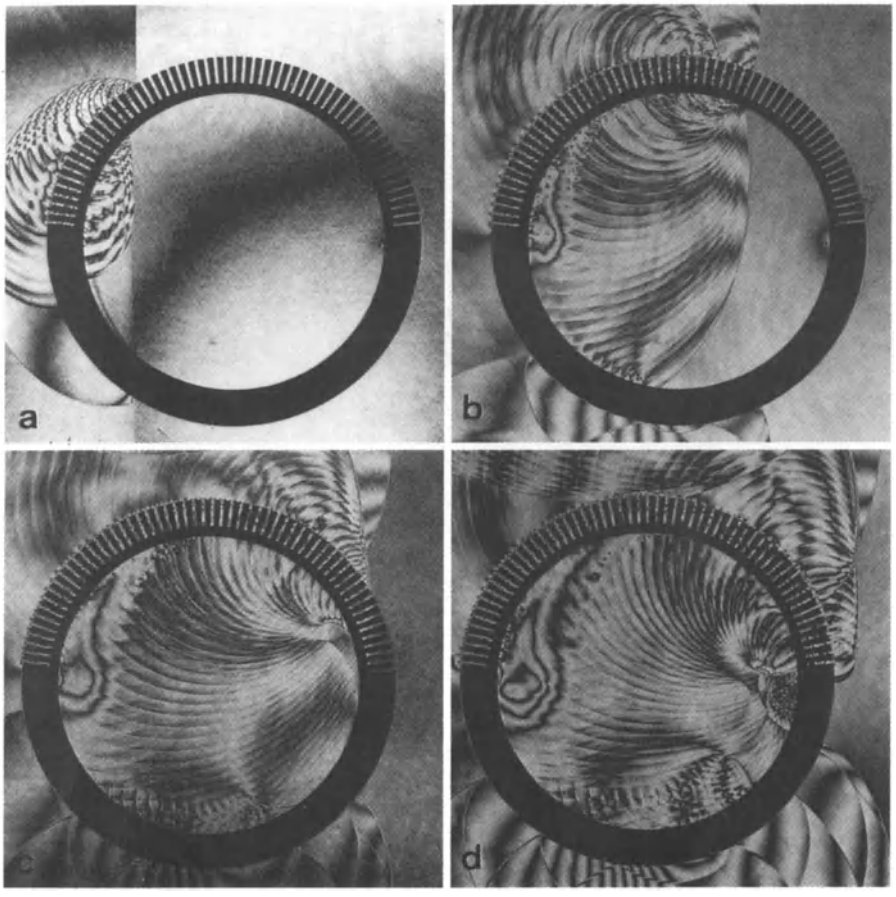

Fig. 4. Shock propagation over a hollow cylinder with slotted surface

4. Shock wave interaction with soap bubbles

In conjunction with studies of shock wave refraction over gaseous interfaces which were either planar or curved, separating gases having different specific heat ratios and sound speeds (Jahn 1958; Henderson and Abdel-Fattah 1978a; 1978b; Benjamin et al. 1992), a holographic interferometric study was made. Most of the flow visualization methods in previous works were Schlieren or shadowgraph. Jahn (1958) used finite fringe interferometry, however, spatial resolution was unfortunately unsatisfactory to understand the isopycnics behind the refracting shock waves.

4.1. Blast wave interaction with a spherical soap bubble

Double exposure holographic interferometry was applied in order to visualize the interaction of a microblast wave with a spherical soap bubble filled with helium gas. The microblast wave was generated in open air by detonating a silver azide pellet which was 10 mg in weight and approximately 0.8 mm dia. and 1.0 mm long. Stuck on the tip of a 0.6 mm dia. optical fibre, the microexplosive was ignited by illuminating it with a Q-switched YAG laser beam of 20 mJ and

8 ns pulse duration. The ignition delay time was not more than the pulse duration of the YAG laser.

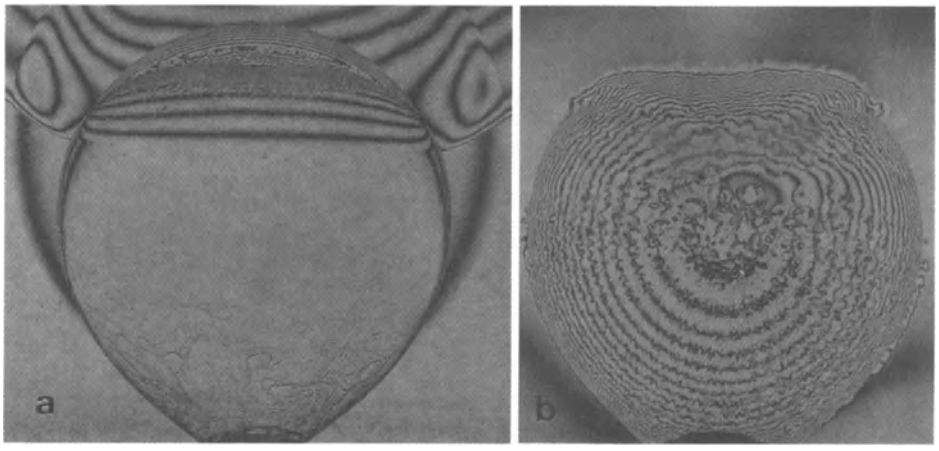

Fig. 5. Interaction of a microblast wave with a soap bubble filled with He

The soap bubble was formed by feeding slowly with slightly pressurized helium from atmospheric pressure, to a diameter of approximately 50 mm. The stand-off distance between the center of the soap bubble and the microexplosive pellet was approximately 90 mm. The overpressure of the microblast wave at this distance was approximately 5 kPa. Fig.5 shows sequential interferograms of the interaction of the microblast wave with the soap bubble.

The propagation speed of the microblast wave being slower than the sound speed in helium, a precursory wave was visible ahead of the blast wave. In this series of experiments it was assumed that the the soap bubble was so thin that the effect of the finite thickness of the soap bubble on the deformation of gaseous interfaces was negligible. The particle velocity induced behind the microblast wave is a maximum just behind the microblast wave and attenuates very quickly. At 15 μs from the microblast wave passage the particle velocity changes its flow direction to the reverse direction. As a result, the deformation of the air/helium interface is not drastic, as seen in Fig.5.

4.2. Shock wave interaction with a cylindrical soap bubble

A soap bubble filled with helium was formed in an approximately 60 mm dia. and 60 mm wide cylindrical shape and set in a 60 mm × 150 mm cross-sectional shock tube. In order to sustain the cylindrical soap bubbles horizontally in the shock tube, 1.0 mm thick and 1.0 mm wide brass rings were stuck on glass plates of the shock tube test section.

Fig.6 shows sequential interferograms of the interaction of a planar shock wave of $M_S = 1.2$ in air with a helium bubble (Nagoya 1994). Upon shock impingement, the front surface of the helium bubble started to deform and precursory waves were visible in front of the diffracting shock wave. The air/helium interface moved with a speed very close to that of the particle velocity behind a shock wave of $M_S = 1.2$. The deformation of the front surface of the interface became enhanced with the lapse of time. The front surface of the air/helium interface was accelerated so that the prevailing acceleration, keeping the pressure nearly identical across the interface,